High Rate Sputtering of Corrosion-Resistant Alloys†

Masaaki NAKA*, Hiroyasu FUJIMORI***, Shuji HANADA****, Ikuo OKAMOTO** and Yoshiaki ARATA**

Abstract

High corrosion-resitant films of amorphous $Fe_{80-X}Cr_XP_{13}C_7$, $Fe_{45}Cr_{30}Mo_5P_{13}C_7$, $Cr_{70}C_{30}$, $Cr_{75}B_{25}$ and $Ti_{75}B_{25}$ were deposited by dc-triode sputtering on water-cooled copper substrate. X-ray diffractometry showed a few diffraction patterns that characterize the amorphous structure for deposited films. High sputtering rate of about 0.1 μm/min was achieved by appling high ion current densities to the sputtering target under 10^{-2} Torr of Ar gas. The high dense Ar plasma ions were produced using a plasma generator.

The microhardness of amorphous $Cr_{70}C_{30}$, $Cr_{75}B_{25}$ and $Ti_{75}B_{25}$ were 1288, 1168 and 1081, respectively. The films, which contain high corrosion resitant alloying elements such as Cr and Ti, show extremely high corrosion resistance, particularly pitting corrosion resitance in IN HCI. The high corrosion resistance of these films is attributable to the enrichment of Cr and Ti in the passive films.

KEY WORDS : (Sputtering) (Corrosion Resistance) (Thin Films) (Surface) (Amorphous Alloys) (Chromium) (Titanium)

1. Introduction

There have been a dramatic increase in vapor quenching studies[1,2]. Sputtering has traditionally been a slow process with deposition rates ranging from 10 to 100 Å/min using a conventional rf-sputtering, and consequently restricted to the preparation of thin films. The recent development of high-rate sputtering techniques has made it to produce thick, homegenous deposits of a variety of materials including metallic amorphous and metastable crystalline alloys. High rate deposition rates of 1 μm/min, for example, have been reported for triode sputtering[3], cylindrical[4] and planar[5] magnetron sputtering and co-evaporation[6] vapor-deposition techniques. Sputtering deposition provides a method of the wide and thick film for corrosion-resistant coating.

This paper describes a high rate dc-triode sputtering apparatus and procedures used to produce thick corrosion-resistant amorphous deposits and corrosion properties of the films.

2. Experimental Procedures

Figure 1 shows the schematic diagram of the present high rate sputtering apparatus. The stainless steel chamber of 20 cm in diameter and 30cm in length is evacuated up to 10^{-8} Torr prior to the filling of a purified Ar gas. The pressure of the Ar gas during sputtering is kept at 10^{-2} Torr with an automatic gas flow controller. High sputtering rate of 0.1 μm/min is achieved by appling high ion current densities to sputtering target. High ion curretnt densities in the triode sputtering apparatus are created by adding large amounts of electrons to the system with a tungsten filament through an independent low voltage

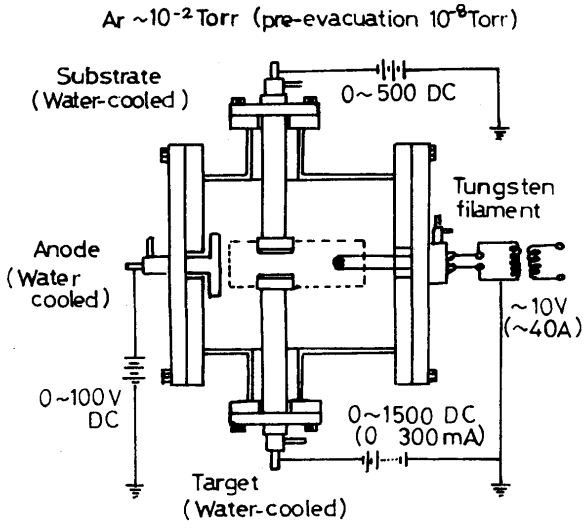

Fig. 1 Schematic diagram of dc-triode sputtering apparatus.

† Received on September 30, 1982

* Associate Professor
** Professor
*** Professor, The Research Institute for Iron, Steel and Other Metals, Tohoku Univesity, Sendai
**** Researh Instructor, The Research Institute for Iron, Steel and Other Metals, Tohoku University, Sendai

Transactions of JWRI is published by Welding Research Institute of Osaka University, Ibaraki, Osaka, Japan

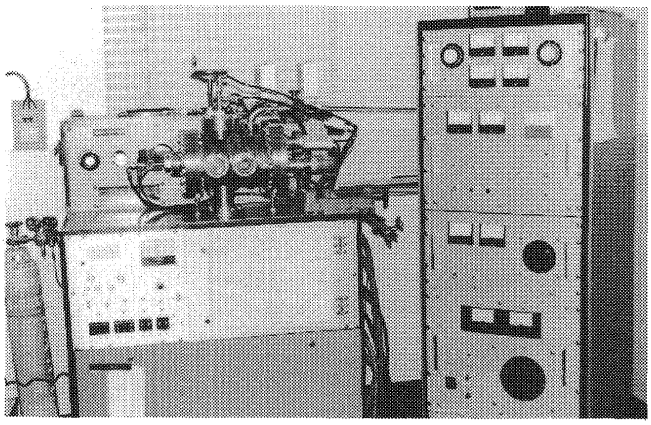

Fig. 2 Sputtering chamber and electric source of dc-triode sputtering apparatus.

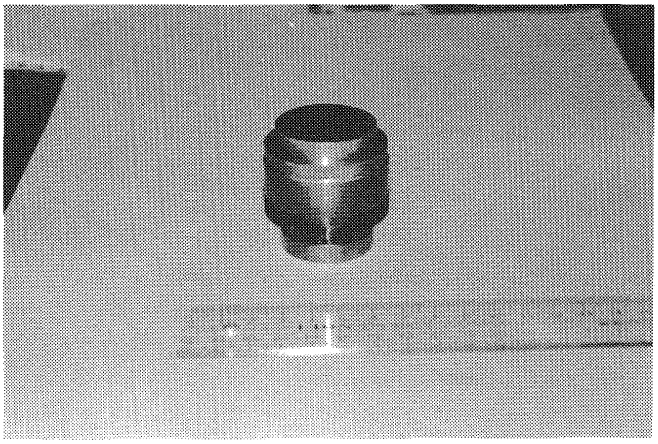

Fig. 3 Substrate holder of dc-triode sputtering apparatus.

10 V of electrical circuit from the filament to the anode. The mother materials to be sputtered are 4 cm in diameter and 8 mm in thickness. Several different types of target such as cast target, compacted target and composite target have been tried[2]. In the present work the cast targets are used. Target cooling is essential because the high energy is delivered during sputtering by the bombarding ions, and cooling removes most of this energy.

The sputtering target is shielded with a cylindrical stainless-steel shielding to avoid the sputtering of the holder. The substrate of copper with the diameter of 4 cm is placed opposite the target with a distance of about 2 cm and water-cooled to promoto the quenching capability of sputtered atoms. Before the sputtering of target, the substrate is sputtered for a few minute by appling a negative potential (400V) to substrate. The sputtering chamber, electric source, substrate holders are shown in **Figs. 2 and 3**, respectively.

The structures of coating films were analysed by X-ray diffraction of Cu · Kα or Co · Kα. The corrosion resistance of the film at room temperature was determined by a potentiodynamic method with a potential sweep rate of 2.5×10^{-3} V/s in 1N HCl, 1N H_2SO_4 and 1N HNO_3. The microhardness was measured using a pyramidal indentor with a 100 gram load. The structure of the coated specimens was examined by scanning or transmission electron microscopy. The sputtering materials were $Fe_{80-X}Cr_XP_{13}C_7$ (X=5 ~20), $Fe_{45}Cr_{30}Mo_5P_{13}C_7$, $Cr_{75}B_{25}$, $Cr_{70}C_{30}$ and $Ti_{75}B_{25}$ alloys. The number attached to respective elements denotes the nominal content in atomic percent.

3. Results and Discussion

Figures 4 to 6 show the crystalline and amorphous X-ray diffraction patterns of mother alloys and deposited films for $Fe_{45}Cr_{30}Mo_5P_{13}C_7$, $Ti_{75}B_{25}$ and

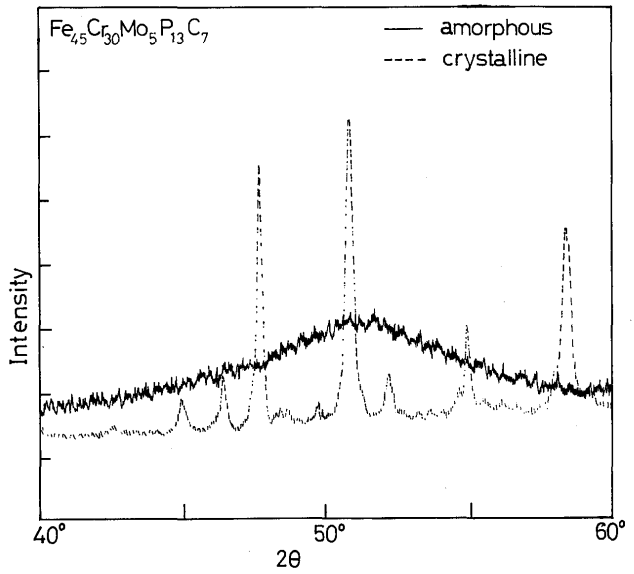

Fig. 4 X-ray diffraction patterns of crystalline and amorphous $Fe_{45}Cr_{30}Mo_5P_{13}C_7$ alloys using Co · Kα.

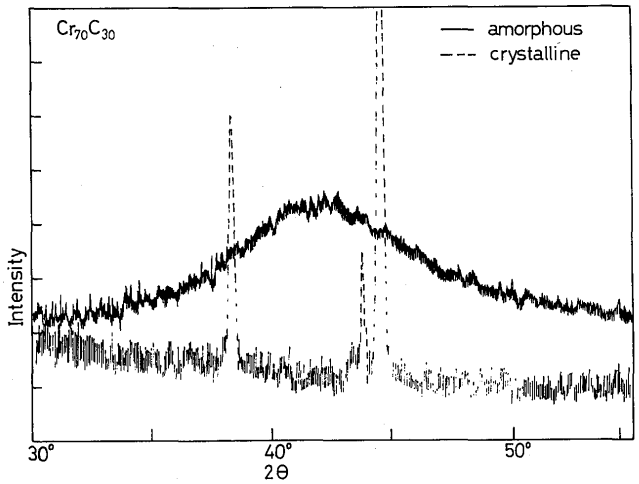

Fig. 5 X-ray diffraction patterns of crystalline and amorphous $Cr_{70}C_{30}$ alloys using Cu · Kα.

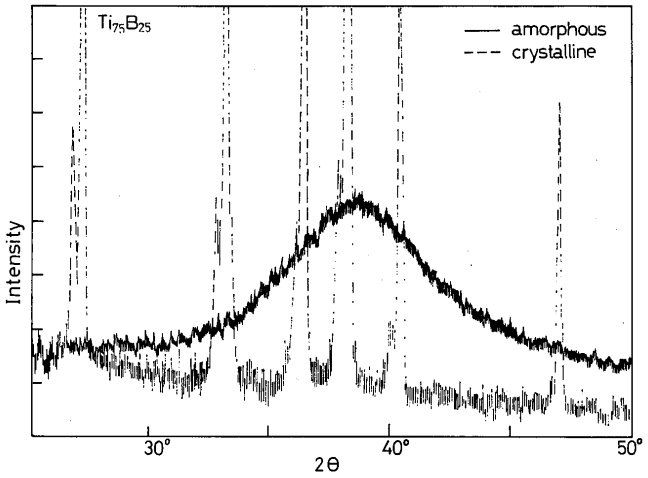

Fig. 6 X-ray diffraction patterns of crystalline and amorphous $Ti_{75}B_{25}$ alloys using Cu · Kα.

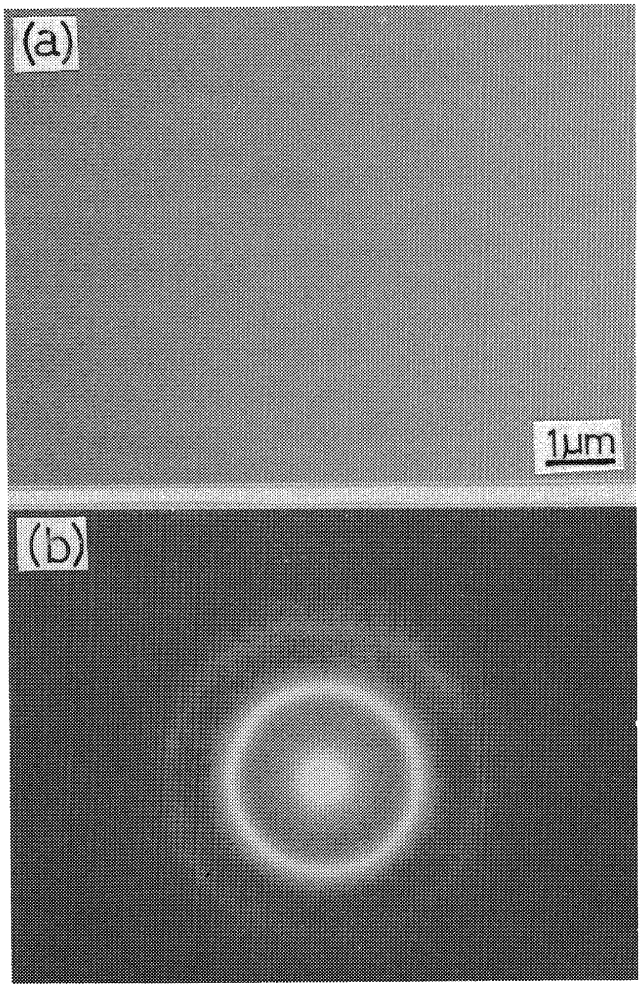

Fig. 7 Transmission electron micrograph (a) and diffraction pattern (b) of amorphous $Fe_{45}Cr_{30}Mo_5P_{13}C_7$ alloy.

$Cr_{70}C_{30}$ alloys, respectively. X-ray diffraction patterns of amorphous structure give only a few diffuse peaks. When alloys contain metalloids such as B, C and P of about 20 at.% or more, the films are deposited to be amorphous. The metalloids stabilize the structure by filling the hole in dense randam packing polyhedron in the amorphous structure[7]. **Fig. 7** represents the typical transmission electron micrograph of amorphous structure for $Fe_{45}Cr_{30}Mo_5P_{13}C_7$ alloy. The bright field image gives the fewtureless contrast and the corresponding diffraction pattern shows only a few diffused haloes.

Table 1 Comparison of microhardness of sputtered amorphous alloys with pure crystalline metals.

Alloy	H_V
$Fe_{60}Cr_{20}P_{13}C_7$	847
$Fe_{45}Cr_{30}Mo_5P_{13}C_7$	882
$Cr_{70}C_{30}$	1288
$Cr_{75}B_{25}$	1168
$Ti_{75}B_{25}$	1081
Cryst. Ti	256
Cryst. Cr	168
Cryst. Nb	129
Cryst. Fe	107
Cryst. Co	150
Cryst. Cu	82

The microhardness of the deposited amorphous films is represented in **Table 1**. The deposited films show the extremely high microhardness. In particular, the hardness of amorphors $Cr_{70}C_{30}$, $Cr_{75}B_{25}$ and $Ti_{75}B_{25}$ and 1288, 1168 and 1081, respectively. The coating of the amorphous films improves the hardness of copper substate (H_V=82). The hardness of amorphous Cr and Ti based alloys are larger than that of crystalline Cr and Ti by factors of four and six, respectively. These high hardness of amorphous alloys arises from the covalent bonding between metals and metalloids that tend to form compounds such as carbide or boride in the crystalline state. The hardness of amorphous $Ti_{75}B_{25}$ is higher than that of another amorphous Ti based alloys containing phosphorus as metalloid[8]. This difference is attributable to the strong chemical bond between metals and boron.

The hardness of amorphous $Fe_{80-X}Cr_XP_{13}C_7$ alloys changes from 720 for $Fe_{75}Cr_5P_{13}C_7$ alloy to 847 for $Fe_{60}Cr_{20}P_{13}C_7$ alloy. The hardness of sputtered amorphous alloys is comparable to that of amorphous Fe-Cr alloys quenched from the liquid state[9]. According to Naka et al.[9], the averaged outer electron concentration of the metallic atoms in amorphous iron alloys plays an important role in the hardness. In other words, alloying effects is mainly confined to the

bonding character of the outer electrons of components.

Anodic polarization curves of amorphous $Ti_{75}B_{25}$ alloy in 1N HCl, 1N H_2SO_4 and 1N HNO_3 are shown in **Fig.8.** The amorphous $Ti_{75}B_{25}$ is extremely stable in various solutions. The outstanding characteristic is that the alloy do not suffer pitting corrosion by anodic polarization, and spontaneous passivation takes place even in 1N HCl. Furthermore, anodic current denisties of amorphous $Ti_{75}B_{25}$ alloy are very low and comparable to that of pure crystalline titanium in various solutions as shown in **Fig.9.** According to Naka et al.[8], the high corrosion resistance of the amorphous titanium alloys is attributable to the passive film of titanium formed on the surface of the alloys. An enrichment of Ti(IV) in the passive film takes place in amorphous titanium alloys and the film composes exclusively hydrated titanium oxide or oxyhydroxide.

Figures 10 and 11 show anodic polarization curves of amorphous $Fe_{60}Cr_{20}P_{13}C_7$, $Cr_{75}B_{25}$ and $Cr_{70}C_{30}$ alloys in 1N HCl. These alloys possess no pitting potentials even in 1N HCl. The anodic current densities of amorphous $Fe_{60}Cr_{20}P_{13}C_7$ alloy are as small as that of pure crystalline chromium in **Fig. 12.** The high corrosion resitance of amorphous Fe-Cr alloys has been interpreted in terms of the rapid formation of a protective passive film in which chromium is remarkably enriched[10]. The uniformity of the passive film is ensured by the amorphous state, that is, the chemical homogeneous stable phase without local defects such as grain boundaries, dislocations and precipitates, on which a stable passive film is unstable to form and on which corrosion initiates. A large amounts of phosphorus, which enhances active dissolution of alloys due to high chemical reactivity, gives rise to the enrichment of chromium at the surface of the alloy. Initial active dissolution of amorphous Fe-Cr alloys preceding the passive film formation is considerably more rapid than that of stainless steel. The higher the reactivity of the alloys the higher is the rate of passive film formation and the better is the protective quality of the film. The rapid dissolution leads to a rapid enrichement of protective passive film. The anodic current density of amorphous $Cr_{75}B_{25}$ is a

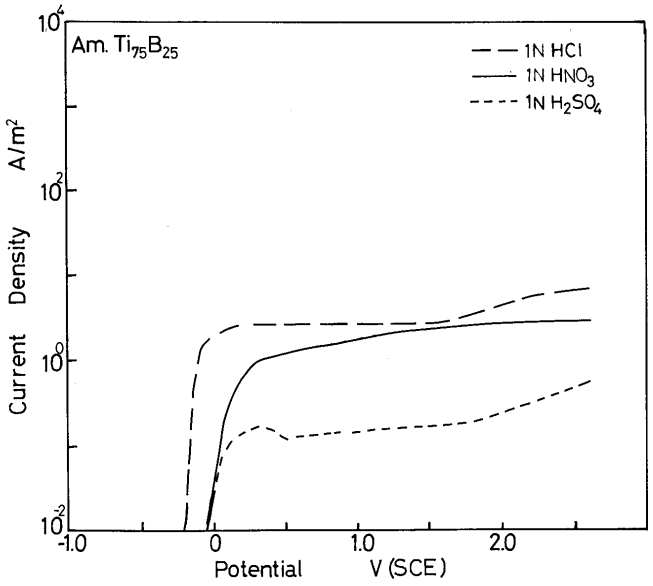

Fig. 8 Potentiodynamic polarization curves of amorphous $Ti_{75}B_{25}$ alloy in 1N HCl, 1N H_2SO_4 and 1N HNO_3.

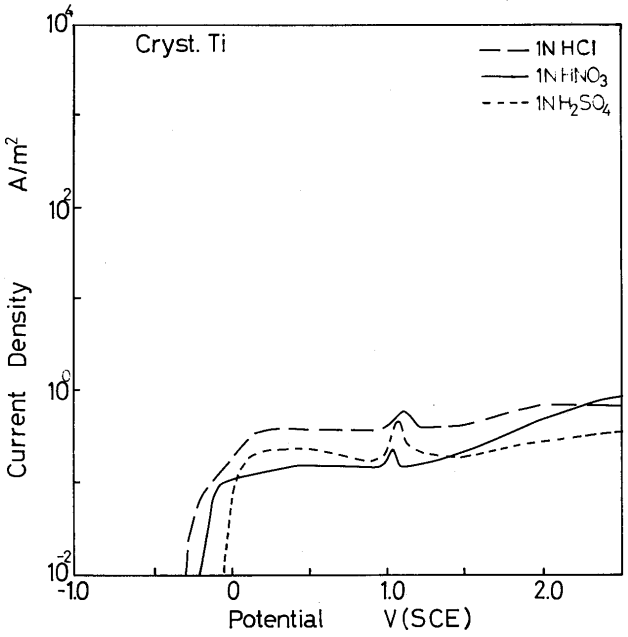

Fig. 9 Potentiodynamic polarization curves of pure crystalline Ti in 1N HCl, 1N H_2SO_4 and 1N HNO_3.

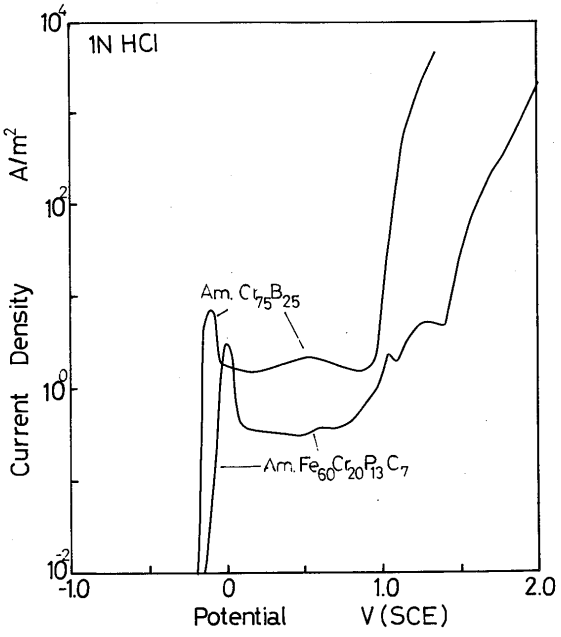

Fig. 10 Potentiodynamic polarization curves of amorphous Fe_{60} $Cr_{20}P_{13}C_7$ and amorphous $Cr_{75}B_{25}$ alloys in 1N HCl.

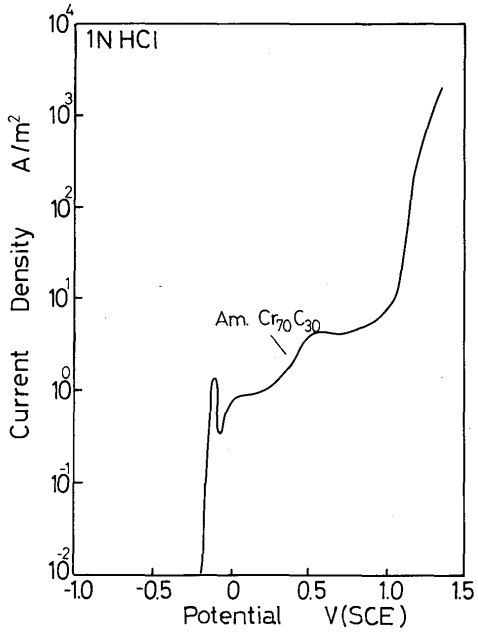

Fig. 11 Potentiodynamic polarization curve of amorphous $Cr_{70}C_{30}$ alloy in 1N HCl.

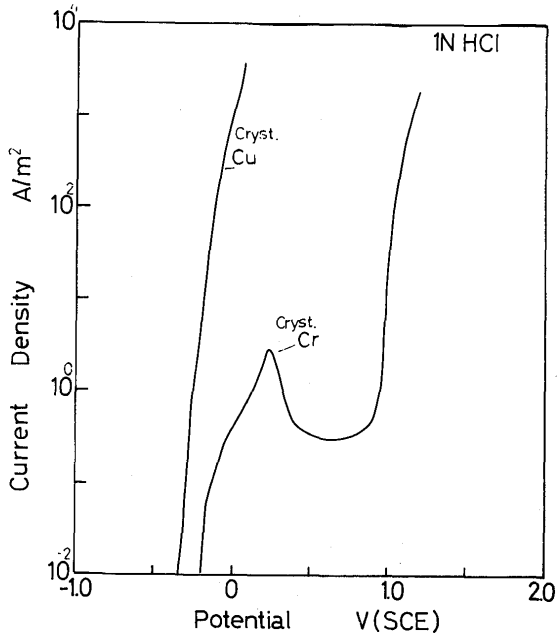

Fig. 12 Potentiodynamic polarization curves of pure crystalline Cu and Cr in 1N HCl.

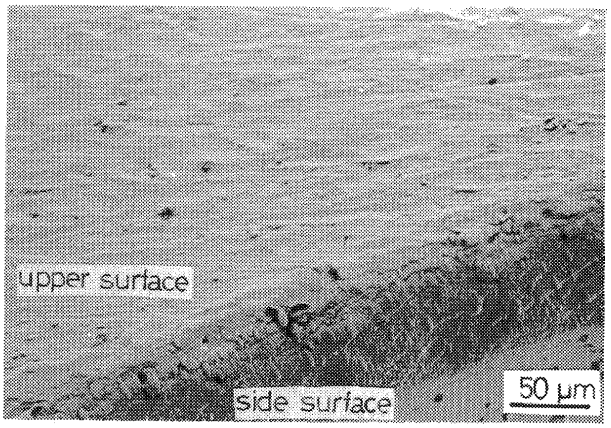

Fig. 13 Surface appearance of amorphous $Fe_{45}Cr_{30}Mo_5P_{13}C_7$ alloy.

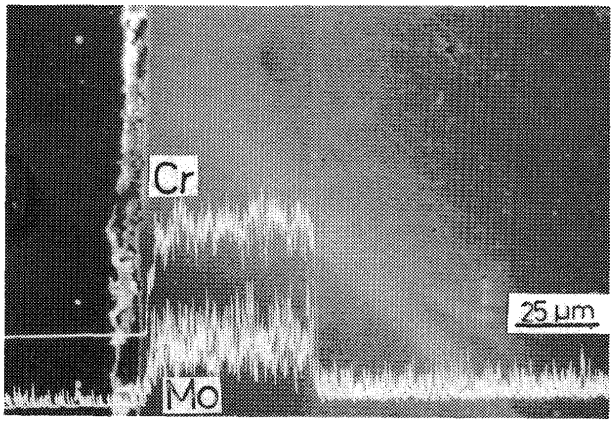

Fig. 14 Line analysis of cross section of sputtered amorphous $Fe_{45}Cr_{30}Mo_5P_{13}C_7$ alloy.

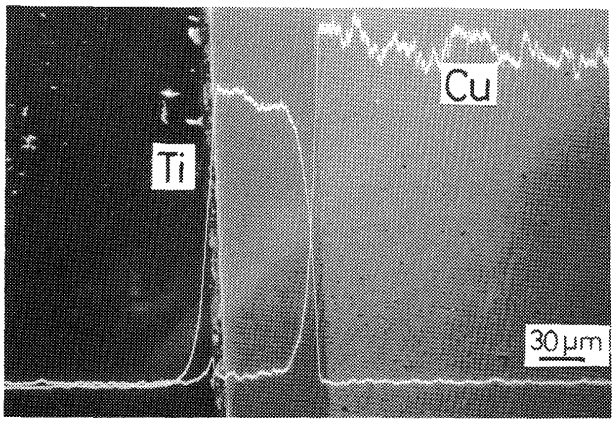

Fig. 15 Line analysis of cross section of sputtered amorphous $Ti_{75}B_{25}$ alloy.

little higher than that of crystalline chromium. In contrast to phosphorus, boron remains in the passive film and retards to enrich the chromium in the passive film. In contrast to the effect of boron, carbon effectively affects the corrosion resitance of amorphous chromium alloys as shown in **Figs. 11 and 12.** The corrosion resitance of crystalline Cu is extremely improved by sputtering the amorphous alloys in **Figs. 10 to 12.**

The coating of the amorphous alloys on the copper substrate is favorable as shown in **Figs. 13 to 15.** The suface appearance of $Fe_{45}Cr_{30}Mo_5P_{13}C_7$ alloy is shown in **Fig. 13.** The films exhibit the uniform distribution of chromium and titanium composition and no defects between the films and copper substrate as shown in **Figs. 14 to 15.**

4. Conclusion

A dc-triode sputtering technique has been applied to produce high corrosion-resitant films. High sputtering rate of about 0.1 μm/min was achieved by appling high ion current densities to the sputtering target under 10^{-2} torr of Ar gas.

Amorphous $Cr_{70}C_{30}$, $Cr_{75}B_{25}$ and $Ti_{75}B_{25}$ films show the extremely high microhardness of 1277, 1168 and 1081, respectively. The high hardness is attributable to the chemical bonding between metals and carbon or boron in amorphous alloys.

Amorphous $Fe_{60}Cr_{20}P_{13}C_7$ alloy exhibits the high corrosion resitance, and are passivated in acid solution containing chloride such as lN HCl. This is attributable to the single phase nature of amorphous structure, and the enrichment of chromium in the passive film. Amorphous $Cr_{70}C_{30}$, $Cr_{75}B_{25}$ and $Ti_{75}B_{25}$ alloys exhibit the extremely high corrosion resistance even in lN HCl. This is attributable to the enrichment of chromium and titanium in the passive film that easily passivated in various solutions.

Acknowledgement

The authors would like to thank Dr. Y. Imai, Emeritus Professor of Tohoku University, for his encouragement to perform this work.

References

1) R. P. Allen, S. D. Dahlgren and M. D. Mertz; Rapidly Quenched Metals Ⅱ, ed. N. J. Grant and B. C. Giesen, MIT Press (1976), 37.
2) S. D. Dahlgren; Rapidly Quenched Metals Ⅲ, ed. B. C. Cantor, Vol. 1, The Metals Society, London(1978), 36.
3) S. D. Dahlgren; Met. Trans. 7A(1967), 1375.
4) J. A. Thornton; J. Vac. Sci. Technol., 15(1978), 171.
5) C. T. Wu. R. T. Kampwirch and J. W. Hafstrom; J. Vac. Sci. Technol., 14(1977), 134.
6) R. H. Hammond, J. Vac. Sci. Technol., 15(1978), 382.
7) D. E. Polk; Acta Met., 20(1972), 485.
8) M. Naka, K. Asami, K. Hashimoto and T. Masumoto; Proc. 4th Int. Conf. on Titanium, ed. H. Kimura and O. Izumi, AIME 1981, 2695.
9) M. Naka, S. Tomizawa, T. Masumoto and T. Watanabe; Rapidly Quenched Metals Ⅱ, ed. N. J. Grant and B. C. Giesen; MIT Press (1976), 273.
10) K. Hashimoto, M. Naka, K. Asami and T. Masumoto; Boshoku Gijitsu, 27(1978), 279.